ALASKA DEPARTMENT OF
ENVIRONMENTAL CONSERVATION

Amendments to:

State Air Quality Control Plan

Volume III: Appendix III.K.13

Alaska Regional Haze State Implementation Plan

2nd Implementation Period

Appendix to Section III.K.13.G

Adopted

July 5, 2022

Mike J. Dunleavy, Governor

Jason W. Brune, Commissioner

(This page serves as a placeholder for two-sided-copying)

Appendix III.K.13.G. Modeling

Contents

Mao, J. & Zheng, Y. (2019). Final report of UAF GEOS.Chen Model support for Regional State Implementation Plan

Kotchenruther, R.A. (2017). The effects of marine vessel fuel sulfur regulations on ambient $PM_{2.5}$ at coastal and near coastal monitoring site in the US.

FINAL REPORT

UAF GEOS-Chem model support for the Regional Haze State Implementation Plan

Jingqiu Mao and Yiqi Zheng

University of Alaska Fairbanks

Date: July 05, 2019

1. Introduction

GEOS-Chem is a global 3-D chemical transport model driven by meteorological input from the Goddard Earth Observing System (GEOS) of the NASA Global Modeling and Assimilation Office (www.geos-chem.org). We use the GEOS-Chem model in this study to understand how regional visibility in Alaska National Parks is affected by local and long-range transport of pollutants. GEOS-Chem model has been widely used for past aircraft campaigns and surface site evaluations, including a number of model evaluations over the Arctic for oxidants [*Mao et al.*, 2010], CO [*Fisher et al.*, 2010], sulfate [*Fisher et al.*, 2011], BC and OC [*Wang et al.*, 2011], and biomass burning emissions [*Alvarado et al.*, 2010].

2. Model setup

We run GEOS-Chem v12.1.0 (https://doi.org/10.5281/zenodo.1553349) for this study. We choose the assimilated meteorological observations from the Goddard Earth Observing System (MERRA-2) of the NASA Global Modeling and Assimilation Office (GMAO). The MERRA-2 meteorological data have 3-h temporal resolution (1-h for surface variables and mixing depths) with $0.5°x0.625°$ horizontal resolution and 72 vertical layers from the surface to 0.01 hPa. We regrid here the meteorological data to $2°x2.5°$ horizontal resolution and 47 vertical layers for input to GEOS-Chem. We emphasize that both 47 and 72 vertical layers have the same grid setup from surface to lower stratosphere (surface to 17 km). The main difference between these two vertical grids is in upper stratosphere and above. Since we are not explicitly resolving stratosphere (unless we run UCX) in this study, we adopt 47 vertical layers for this study. The model is initialized with a 6-month simulation from January of 2015 to June of 2015 with $4°x5°$ resolution, and a 6-month simulation from July of 2015 to December of 2015 with $2°x2.5°$ resolution. The sensitivity run (Zero Out Rest of World run) applies the same restart file from June of 2015 as the base run, and then spins up with a 6-month simulation from July of 2015 to December of 2015 with $2°x2.5°$ resolution and its own configuration. Both base run and sensitivity run were conducted on Research Computing Systems (RCS) at the Geophysical Institute of University Alaska Fairbanks.

All GEOS-Chem emissions are configured at run-time using the HEMCO module described by *Keller et al.* [2014]. HEMCO allows users to mix and match inventories from the GEOS-Chem library or add their own, apply scaling factors, overlay and mask inventories, etc. without having to edit or compile the code.

2.1 Base run

The base run in the model applies the following anthropogenic emissions:

- the US (NEI11v1) from EPA [2014], as implemented by *Travis et al.* [2016]

- the Canada Air Pollutant Emission Inventory (APEI) provided by Environment Canada (http://ec.gc.ca/inrp-npri/donnees-data/ap/index.cfm?lang=En)

- the Europe (EMEP) emission is from EMEP [2014] as implemented by *van Donkelaar et al.* [2008].

- The East Asia MIX inventory implemented by *Li et al.* [2014].

- Africa for 2006 and 2013 (DICE-Africa inventory of *Marais and Wiedinmyer* [2016].

- The rest of the world use the Community Emissions Data System (CEDS) emission inventory (http://www.globalchange.umd.edu/ceds/) [*Hoesly et al.*, 2018].

- Aircraft, AEIC Aircraft emissions are from the AEIC inventory[*Stettler et al.*, 2011].

- Shipping emission is based on CEDS and EMEP, as mentioned above.

We have also included other emission sources including:

- Biomass, the biomass burning emissions use the year-specific daily mean GFED4s (Global Fire Emissions Database with small fires) inventory [*van der Werf et al.*, 2010],
- Volcanic SO2 Eruptive and non-eruptive volcanic SO2 emissions for individual years are from the AEROCOM data base originally developed by Thomas Diehl and implemented into GEOS-Chem by Fisher et al. [2011].
- Biogenic VOC emissions in GEOS-Chem are from the MEGAN v2.1 inventory of [*Guenther et al.*, 2012].

For secondary organic aerosol scheme, we applied simple_SOA algorithm for this study (http://wiki.seas.harvard.edu/geos-chem/index.php/Secondary_organic_aerosols#Simple_SOA_scheme). The OM/OC ratio for SOA in the model is set to be 2.1

2.2 Zero Out Rest of World run (ZROW)

To evaluate the impact of international emissions, we conducted a sensitivity run, Zero Out Rest of World run (ZROW). In this case, we set all anthropogenic emissions outside the U.S. set to zero. This involves two mask files provided by Ramboll, including:

1. **AlaskaHawaiiMask.0.5DegRes.nc** is a mask that will zero-out emissions everywhere except in Alaska and Hawaii. This mask can be applied to the global CEDS inventory in the ZROW simulation.
2. **AK_CONUS_ShippingAircraft.geos.1x1** is a mask that will zero-out emissions everywhere except for continental US and Alaska. This mask can be applied to shipping, aircraft, and global anthropogenic C_2H_6 emissions in the ZROW simulation.

This mask can be illustrated by the plot below, where anthropogenic emissions outside of the red boxes are considered "international".

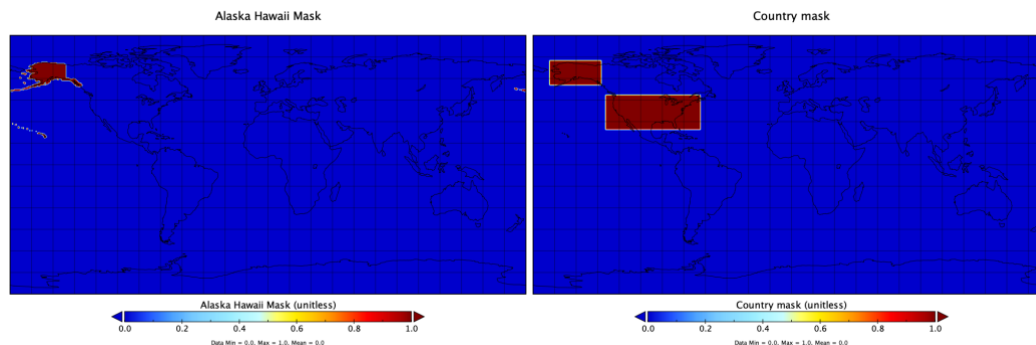*Figure 1 Masks applied in this study for ZROW run. The left plot is the mask applied by the file AlaskaHawaiiMask.0.5DegRes.nc and the right plot is the mask applied by the file AK_CONUS_ShippingAircraft.geos.1x1.*

3. Model results

The model simulations are evaluated by observations from four monitoring sites in the Interagency Monitoring of Protected Visual Environments (IMPROVE) network (Denali National Park, 63.72333, -148.9675, DENA1; Kenai Peninsula Borough, 60.012315, -151.711491, KPBO1; Simeonof, 55.32552 -160.50626, SIME1; Trapper Creek-Denali, 62.31526, -150.31555, TRCR1). The evaluated species include sulfate, nitrate, ammonium, organic aerosols and black carbon for a whole annual cycle (12 months) for the year of 2016.

The mass concentration reported here are in units of [ug/m3]. The mass concentration reported here are converted from volume ratio (mol/mol) using the following equation:

Mass concentration [ug/m3] = SpeciesConc [mol/mol] * (MW/MW_air) * AD / (DXYP*BXHEIGHT) * 10^9

Where AD is Air mass in grid cell [kg], DXYP is the surface area of grid cell[m2], BXHEIGHT is the height of box [m], and MW is the molecular weight. MW for NO3 is 62 g/mol, for SO4 is 96 g/mol, for BCPI, BCPO, OCPI and OCPO is 12 g/mol, for SOAS and SOAP is 150 g/mol.

DENA1, TRCR1, KPBO1, and SIME1 are compared to corresponding model bottom layer grid. In GEOS-Chem model, EC has two tracers, hydrophobic (BCPO) and hydrophilic (BCPI), with an e-folding time of 1 day for conversion from BCPO to BCPI. Similarly, OC has two tracers from primary emission, hydrophobic (OCPO) and hydrophilic (OCPI). In addition, we have two additional tracers for secondary organic aerosol (SOAS and SOAP).

Table 1 IMPROVE and model variables for comparison

IMPROVE parameter	IMPROVE code	Model variable
Sulfate (Fine)	SO4f	SO4
Nitrate (Fine)	NO3f	NO3
Carbon, Elemental Total (Fine)	ECf	BCPI + BCPO
Carbon, Organic Total (Fine)	OCf	OCPI + OCPO + SOAS/2.1 + SOAP/2.1

3.1 Model base run

We show in Figures 2-5 that the GEOS-Chem base run agree reasonably well with IMPROVE observations from the monthly average comparisons. To further investigate the day-to-day variability, we compared daily average concentrations of OC and sulfate between IMPROVE and GEOS-Chem in Figures 6-7.

Figure 2 shows that all four IMPROVE sites show an enhancement of OC during the summer, suggesting the important contribution of wildfires and biogenic SOA for OC. The GEOS-Chem

base run reproduces the magnitude and seasonal variation of organic carbon. Among all four sites, OC appears to account for the majority of aerosol mass in fine particles.

Figure 3 shows that all four IMPROVE sites tend to have highest sulfate during the summer. This seasonality is well captured by our GEOS-Chem base run. We also find from Figure 2 that the base run tends to overestimate sulfate throughout the year by on average 30-60%, roughly 0.2-0.3 ug/m^3.

We find from Figure 4 that the base run tends to underestimate nitrate. This could be either duo to the misrepresentation of model chemistry on nitrate, or other processes in the model including transport and emissions. As the nitrate aerosol contributes little to total aerosol mass (~0.1 ug/m^3), this underestimate is considered to be of minor importance for estimate of aerosol mass.

In contrast to nitrate, model tends to significantly overestimate elemental carbon, pointing to issues in model on black carbon scavenging.

We also find from the daily comparison (Figures 6-7) show that model can largely capture the OC variability from IMPROVE data, while tend to overestimate sulfate for episodic events.

3.2 Zero Out Rest of World run (ZROW)
Figures 2-5 also show the model results with ZROW runs, along with the base run and observations from IMPROVE network.
We show from Figure 2 that for organic carbon, the difference between base run and ZROW is rather small during summer when wildfires and biogenic SOA dominate organic carbon in Alaska. This suggests a relatively minor role of international transport on organic carbon during the summer, accounting for 10% of OC.

In contrast to OC, the sulfate concentrations in ZROW run is significantly lower than that in the base run, by on average 40-50% (~0.2 ug/m^3). In fact, sulfate in ZROW simulation is in much better agreement with IMPROVE observations, compared to the base run. This suggests that model may largely overestimate the contribution of sulfate from international sources. We find similar overestimate of elemental carbon by the model, and a much better agreement with ZROW run. It is possible that model may overestimate the contribution of EC from international sources by ~0.1 ug/m^3.
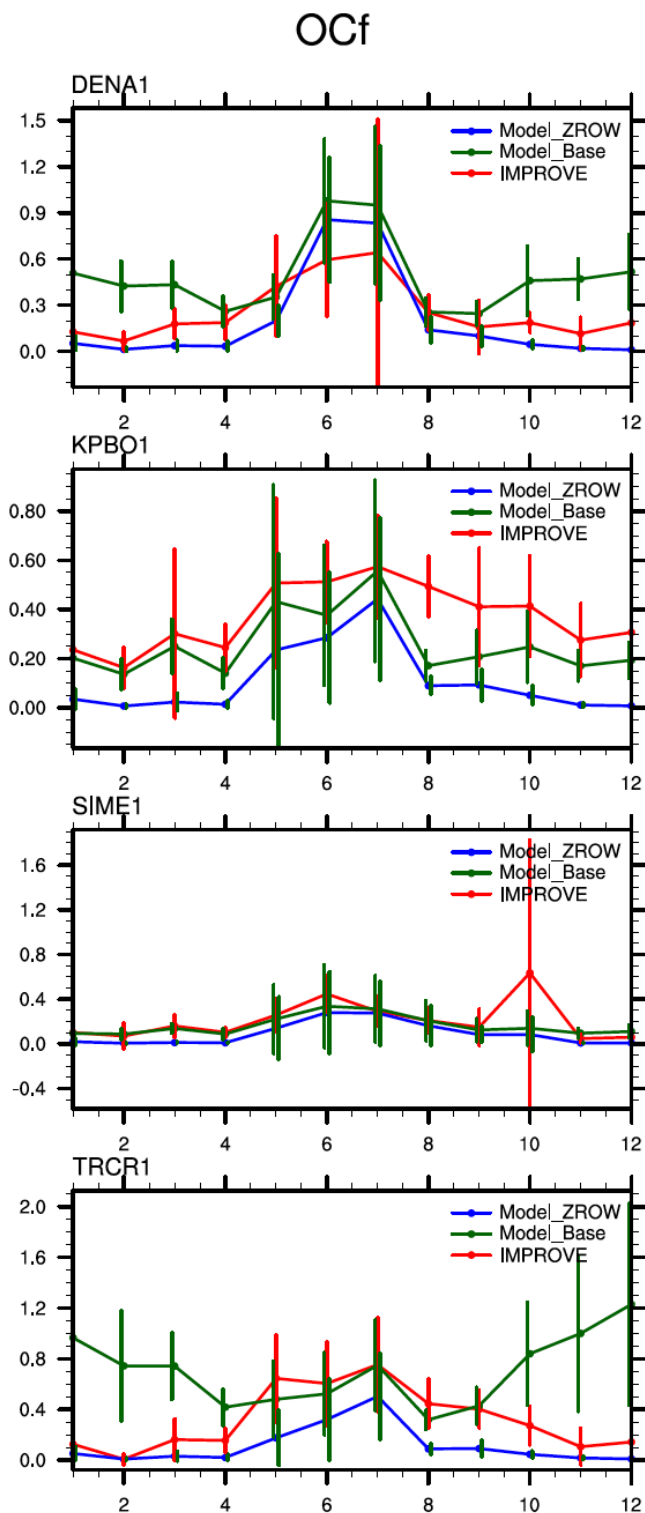
Figure 2 Observed and modeled seasonal cycles of surface OC concentrations at four IMPROVE sites (DENA1, KPBO1, SIME1, TRCR1) in Alaska for the year of 2016. Model simulations include a base GEOS-Chem run (green) and a sensitivity GEOS-Chem run (blue).
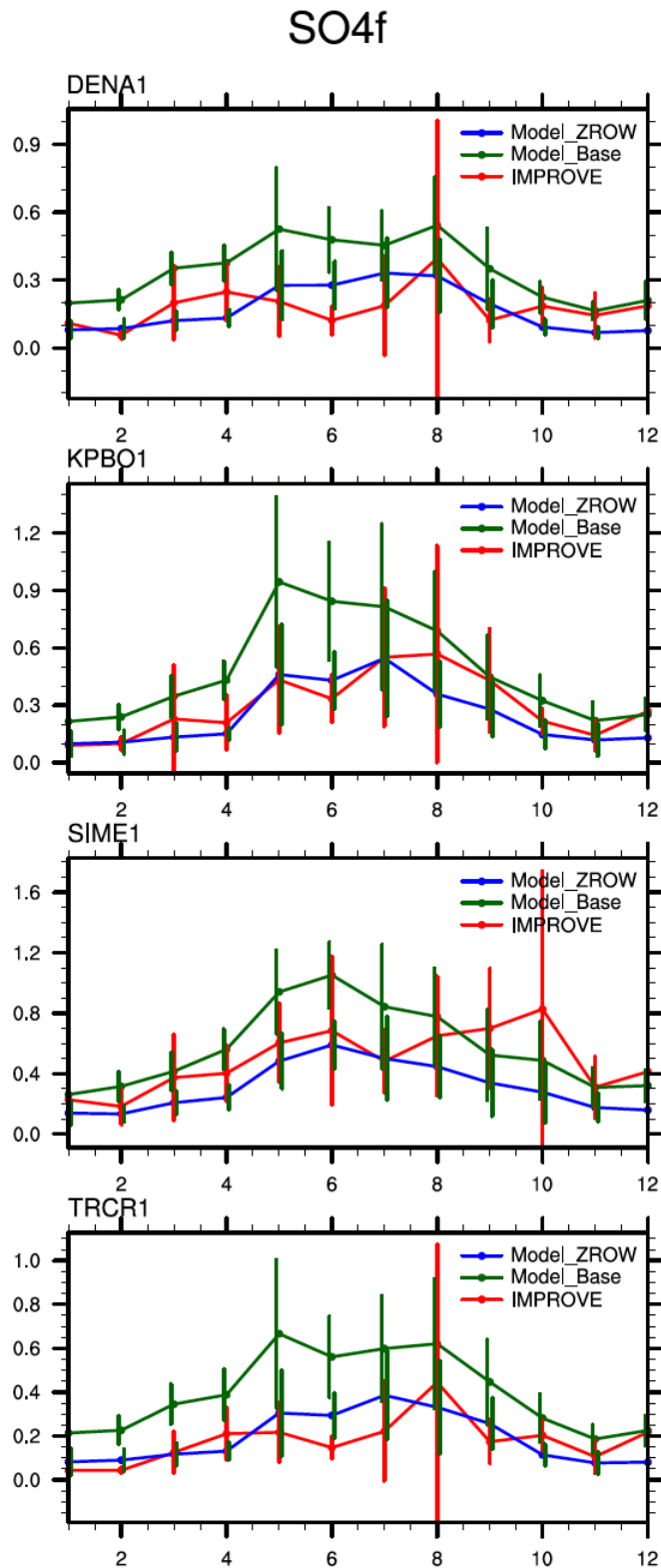
Figure 3 Observed and modeled seasonal cycles of surface sulfate concentrations at four IMPROVE sites (DENA1, KPBO1, SIME1, TRCR1) in Alaska for the year of 2016. Model simulations include a base GEOS-Chem run (green) and a sensitivity GEOS-Chem run (blue).

NO3f

Observed and modeled seasonal cycles of surface nitrate concentrations at four IMPROVE sites (DENA1, KPBO1, SIME1, TRCR1) in Alaska for the year of 2016. Model simulations include a base GEOS-Chem run (green) and a sensitivity GEOS-Chem run (blue).
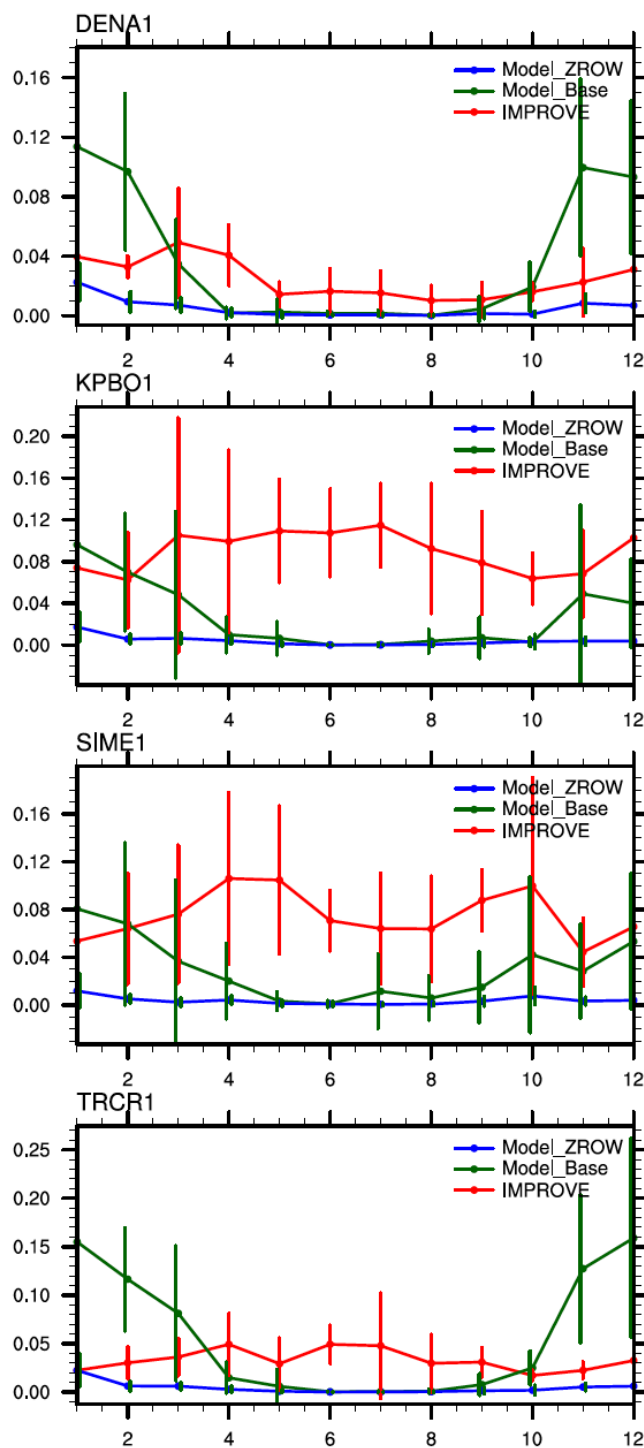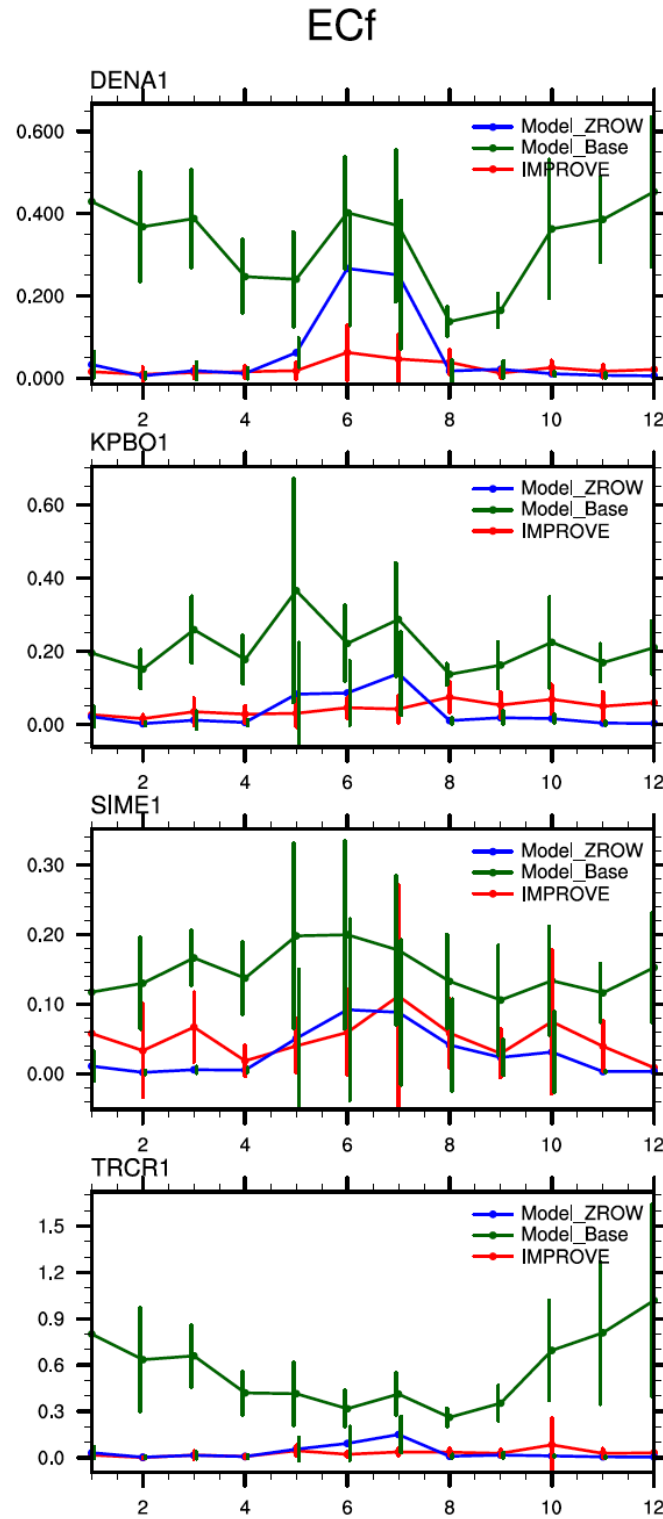
Figure 5 Observed and modeled seasonal cycles of surface EC concentrations at four IMPROVE sites (DENA1, KPBO1, SIME1, TRCR1) in Alaska for the year of 2016. Model simulations include a base GEOS-Chem run (green) and a sensitivity GEOS-Chem run (blue).

Figure 6 Daily averaged concentrations of organic carbon measured by IMPROVE network and simulated by GEOS-Chem model for four sites in Alaska for the year of 2016. Model simulations include a base GEOS-Chem run (green) and a sensitivity GEOS-Chem run (blue).

Figure 7 Daily averaged concentrations of sulfate aerosol measured by IMPROVE network and simulated by GEOS-Chem model for four sites in Alaska for the year of 2016. Model simulations include a base GEOS-Chem run (green) and a sensitivity GEOS-Chem run (blue).
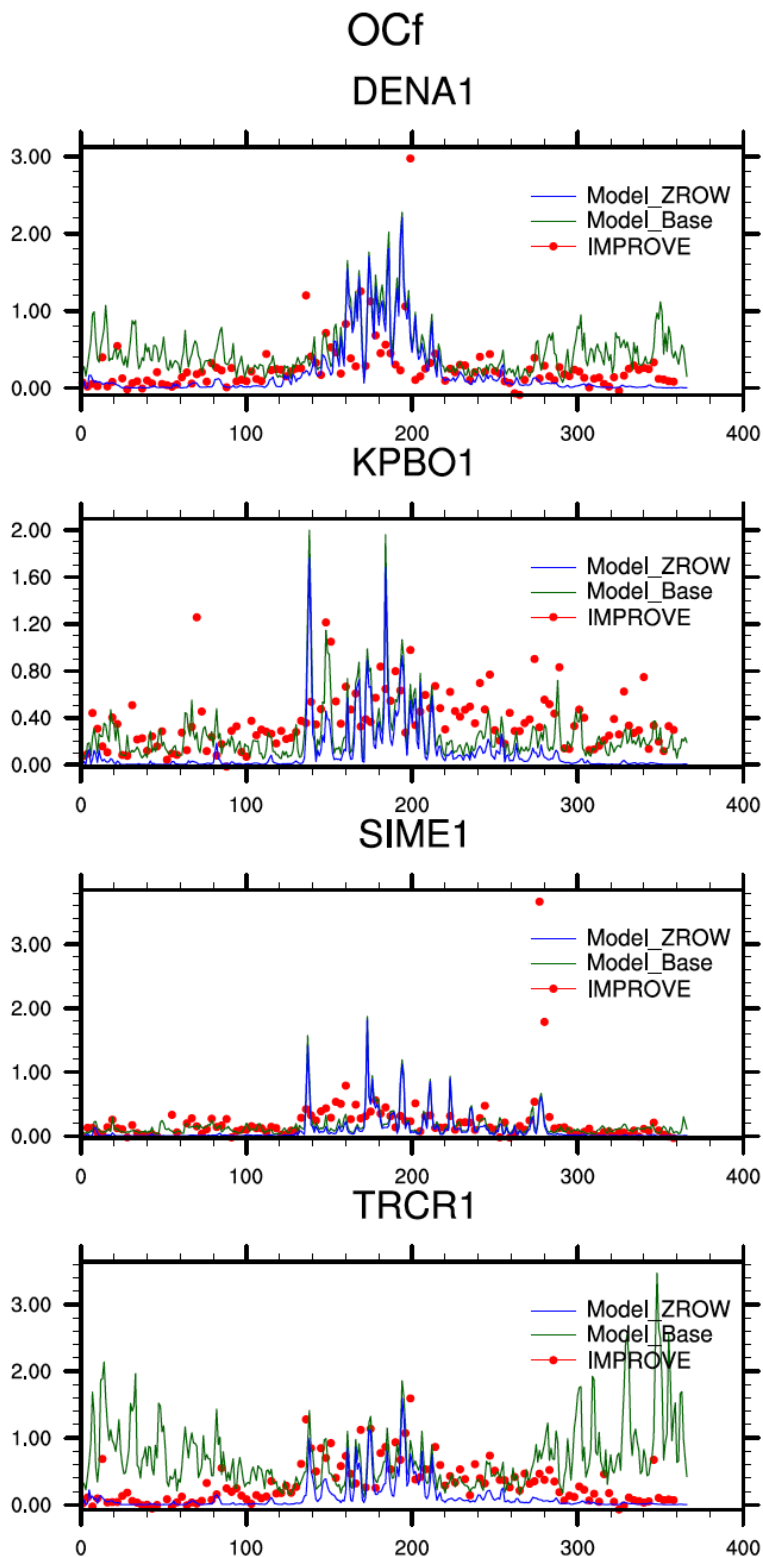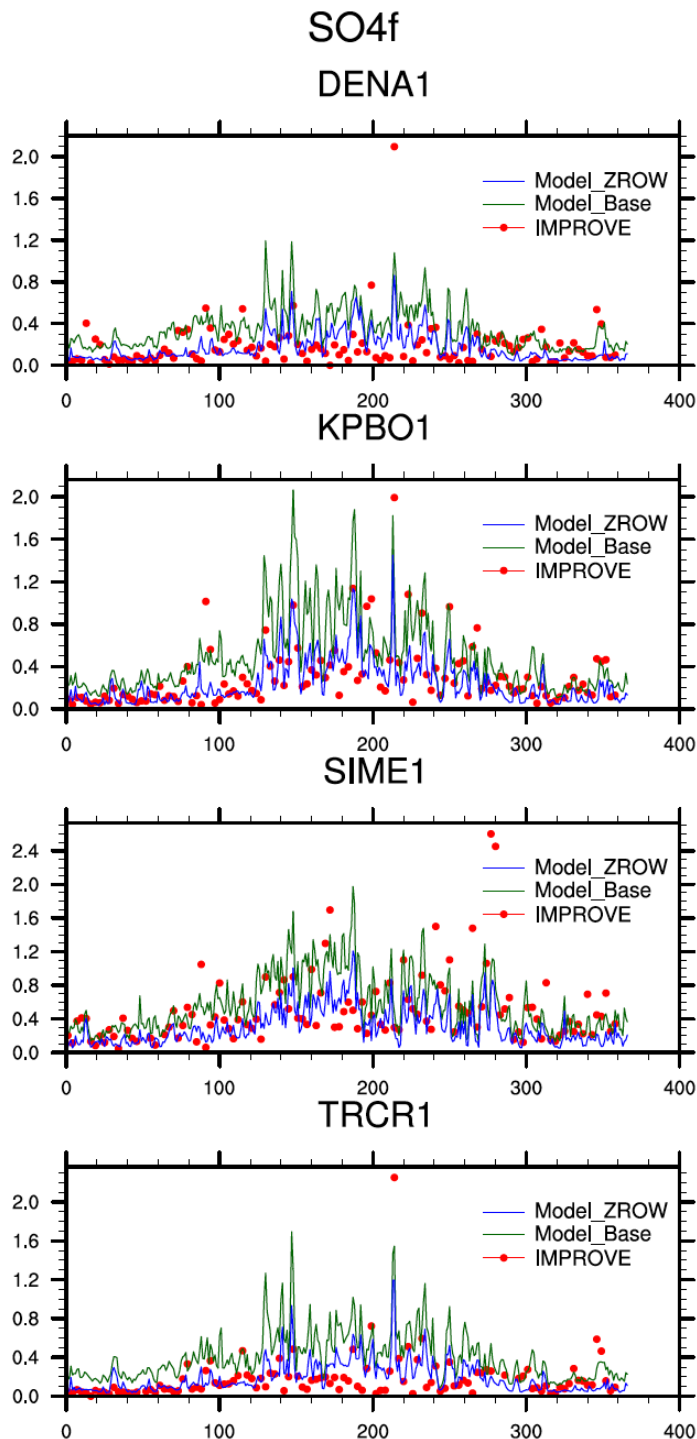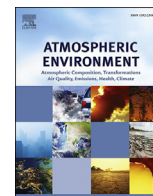
Reference

Alvarado, M. J., et al. (2010), Nitrogen oxides and PAN in plumes from boreal fires during ARCTAS-B and their impact on ozone: an integrated analysis of aircraft and satellite observations, *Atmos. Chem. Phys.*, *10*(20), 9739-9760, doi:10.5194/acp-10-9739-2010.

Fisher, J. A., et al. (2010), Source attribution and interannual variability of Arctic pollution in spring constrained by aircraft (ARCTAS, ARCPAC) and satellite (AIRS) observations of carbon monoxide, *Atmos. Chem. Phys.*, *10*(3), 977-996, doi:10.5194/acp-10-977-2010.

Fisher, J. A., et al. (2011), Sources, distribution, and acidity of sulfate–ammonium aerosol in the Arctic in winter–spring, *Atmos. Environ.*, *45*(39), 7301-7318, doi:10.1016/j.atmosenv.2011.08.030.

Guenther, A. B., X. Jiang, C. L. Heald, T. Sakulyanontvittaya, T. Duhl, L. K. Emmons, and X. Wang (2012), The Model of Emissions of Gases and Aerosols from Nature version 2.1 (MEGAN2.1): an extended and updated framework for modeling biogenic emissions, *Geosci. Model Dev.*, *5*(6), 1471-1492, doi:10.5194/gmd-5-1471-2012.

Hoesly, R. M., et al. (2018), Historical (1750–2014) anthropogenic emissions of reactive gases and aerosols from the Community Emissions Data System (CEDS), *Geosci. Model Dev.*, *11*(1), 369-408, doi:10.5194/gmd-11-369-2018.

Keller, C. A., M. S. Long, R. M. Yantosca, A. M. Da Silva, S. Pawson, and D. J. Jacob (2014), HEMCO v1.0: a versatile, ESMF-compliant component for calculating emissions in atmospheric models, *Geosci. Model Dev.*, *7*(4), 1409-1417, doi:10.5194/gmd-7-1409-2014.

Li, M., et al. (2014), Mapping Asian anthropogenic emissions of non-methane volatile organic compounds to multiple chemical mechanisms, *Atmos. Chem. Phys.*, *14*(11), 5617-5638, doi:10.5194/acp-14-5617-2014.

Mao, J., et al. (2010), Chemistry of hydrogen oxide radicals (HOx) in the Arctic troposphere in spring, *Atmos. Chem. Phys.*, *10*(13), 5823-5838, doi:10.5194/acp-10-5823-2010.

Marais, E. A., and C. Wiedinmyer (2016), Air Quality Impact of Diffuse and Inefficient Combustion Emissions in Africa (DICE-Africa), *Environ. Sci. Technol.*, *50*(19), 10739-10745, doi:10.1021/acs.est.6b02602.

Stettler, M. E. J., S. Eastham, and S. R. H. Barrett (2011), Air quality and public health impacts of UK airports. Part I: Emissions, *Atmospheric Environment*, *45*(31), 5415-5424, doi:https://doi.org/10.1016/j.atmosenv.2011.07.012.

Travis, K. R., et al. (2016), Why do models overestimate surface ozone in the Southeast United States?, *Atmos. Chem. Phys.*, *16*(21), 13561-13577, doi:10.5194/acp-16-13561-2016.

van der Werf, G. R., J. T. Randerson, L. Giglio, G. J. Collatz, M. Mu, P. S. Kasibhatla, D. C. Morton, R. S. DeFries, Y. Jin, and T. T. van Leeuwen (2010), Global fire emissions and the contribution of deforestation, savanna, forest, agricultural, and peat fires (1997–2009), *Atmos. Chem. Phys.*, *10*(23), 11707-11735, doi:10.5194/acp-10-11707-2010.

van Donkelaar, A., et al. (2008), Analysis of aircraft and satellite measurements from the Intercontinental Chemical Transport Experiment (INTEX-B) to quantify long-range transport of East Asian sulfur to Canada, *Atmos. Chem. Phys.*, *8*(11), 2999-3014.

Wang, Q., et al. (2011), Sources of carbonaceous aerosols and deposited black carbon in the Arctic in winter-spring: implications for radiative forcing, *Atmos. Chem. Phys.*, *11*(23), 12453-12473, doi:10.5194/acp-11-12453-2011.

The effects of marine vessel fuel sulfur regulations on ambient PM$_{2.5}$ at coastal and near coastal monitoring sites in the U.S.

Robert A. Kotchenruther

U.S. Environmental Protection Agency Region 10, Office of Environmental Review and Assessment, 1200 Sixth Avenue, Mailstop OEA-140, Seattle, WA, 98101, USA

HIGHLIGHTS

- PM$_{2.5}$ source apportionment was performed for 22 sites in U.S. Coastal States.
- PM$_{2.5}$ impacts from marine vessel residual fuel oil combustion were quantified.
- Ambient effects from implementing an emissions control area were determined.
- Reductions in PM$_{2.5}$ from residual fuel oil combustion aligned with regulations.
- Significant reductions in PM$_{2.5}$ from residual fuel oil combustion were found.

ARTICLE INFO

ABSTRACT

In August of 2012 the U.S. began implementing fuel sulfur limits on certain large commercial marine vessels within 200 nautical miles (nm) of its coasts as part of a North American Emissions Control Area (NA-ECA). The NA-ECA limited fuel sulfur use in these vessels to below 1% in 2012 and to below 0.1% starting in 2015. This work uses ambient PM$_{2.5}$ monitoring data from the U.S. IMPROVE network and Positive Matrix Factorization (PMF) receptor modeling to assess the effectiveness of the NA-ECA at reducing ambient PM$_{2.5}$ from high-sulfur residual fuel oil (RFO) use. RFO combustion emissions of PM$_{2.5}$ are known to have a fairly unique vanadium (V) and nickel (Ni) trace metal signature. To determine if IMPROVE sites were affected by residual fuel oil combustion, V and Ni data from 65 IMPROVE sites in coastal States of the U.S. were analyzed from 2010 to 2011, the two years prior to NA-ECA implementation. 22 of these IMPROVE sites had a V and Ni correlation coefficient (r^2) greater than 0.65 and were selected for further analysis by PMF. The slopes of the correlations between V and Ni at these 22 sites ranged from 2.2 to 4.1, consistent with reported V:Ni emission ratios from RFO combustion. Each of the 22 IMPROVE sites was modeled independently with PMF, using the available PM$_{2.5}$ chemical speciation data from 2010 to 2015. PMF model solutions for the 22 sites contained from 5 to 9 factors, depending on the site. At every site a PMF factor was identified that was associated with RFO combustion, however, 9 sites had PMF factors where RFO combustion was mixed with other aerosol sources. For the remaining 13 sites, PM$_{2.5}$ from RFO combustion was analyzed for three time periods; 2010−2011 representing the time period prior to the NA-ECA implementation (pre-NA-ECA), 2013−2014 representing the time period where fuel sulfur was limited to 1.0% (NA-ECA 1.0% S), and 2015 representing the time period where fuel sulfur was limited to 0.1% (NA-ECA 0.1% S). All 13 sites indicated statistically significant reductions in the contribution of RFO combustion to PM$_{2.5}$ between the pre-NA-ECA period and the two periods of fuel sulfur control. The average decrease in annual average PM$_{2.5}$ from RFO combustion from the pre-NA-ECA to NA-ECA 1% S period was 50.2% (range, 29.0%–65.4%) and from the pre-NA-ECA to NA-ECA 0.1% S period was 74.1% (range, 33.0%–90.4%).

Published by Elsevier Ltd.

1. Introduction

Human exposure to fine particulate matter (PM$_{2.5}$, particles with aerodynamic diameter <2.5 μm) has been linked to cardiovascular and pulmonary disease (Künzli et al., 2005), and lung cancer and

E-mail address: Kotchenruther.Robert@epa.gov.

premature mortality (Pope and Dockery, 2006). Anthropogenic emissions of $PM_{2.5}$ also play a role in climate forcing (IPCC, 2014) and deposition of anthropogenic PM can have adverse effects on ecosystem health (Geiser et al., 2010).

Examining air emissions from large commercial marine vessels (CMVs) has been an active area of investigation because these sources typically burn residual fuel oil (RFO), which has a very high sulfur content and high emissions of $PM_{2.5}$, SO_2, and NO_x (Moldanova et al., 2009), and also because CMVs are mobile sources impacting both urban areas and remote coastal areas that have few other direct sources of anthropogenic emissions. RFO is one of several products produced from oil refinery residuum, the residue left over after crude oil distillation. Environmental regulations in developed countries have contributed to a significant decline in on-shore applications of RFO as a fuel source. Excluding maritime applications, between 1986 and 2010 the use of RFO as a fuel source in OECD countries has declined by nearly 70% (Ramberg and Van Vactor, 2014). However, until recently, RFO use as a fuel source for CMVs in most areas of the world has been unregulated, and during the same 1986 to 2010 period RFO use as a marine fuel has increased by about 100% (Ramberg and Van Vactor, 2014).

Globally, approximately 60,000 cardiopulmonary and lung cancer deaths annually have been attributed to exposure to marine vessel emissions (Corbett et al., 2007). Regulating marine vessel fuel sulfur content is a typical approach to reducing emissions. Previous studies have shown that significant reductions in $PM_{2.5}$ and SO_2 occur when ocean going vessels switch from high to low sulfur fuels (Kasper et al., 2007; Khan et al., 2012) and Winebrake et al. (2009) have shown that significant reductions in premature mortality from marine vessel emissions can be achieved by regulating fuel sulfur content below the assumed uncontrolled fuel sulfur content of 2.7%.

Concerns over health and ecological effects of marine vessel emissions led the United States (U.S.) and Canadian governments in 2009 to propose to the International Maritime Organization (IMO) the inclusion of North America in an Emissions Control Area (ECA). In March of 2010 the IMO amended the International Convention for the Prevention of Pollution from Ships (MARPOL) to designate specific portions of North American waters as an ECA (U.S. EPA, 2010). Other existing ECAs include the Baltic Sea and North Sea. Beginning in August 2012, the North American ECA (NA-ECA) required marine vessels within 200 nautical miles (nm) of North American coasts, in waters subject to U.S. and Canadian jurisdiction, to use fuels with sulfur content below 10,000 ppm (1%). Starting in 2015 the NA-ECA required a 0.1% fuel sulfur limit in the designated coastal regions. IMO MARPOL regulations have also set a worldwide fuel sulfur limit of 3.5% starting in 2012, and 0.5% starting in 2020.

Regionally within the U.S., in July 2009 the State of California (CA) implemented their Ocean-Going Vessel Clean Fuel Regulation (CA-CFR, http://www.arb.ca.gov/ports/marinevess/ogv.htm). Phase I of the regulation became effective July 1, 2009 and required ocean-going vessels within 24 nm of the CA coast to use distillate fuels with sulfur content at or below 1.5% and after August 1, 2012 to use distillate fuels at or below 1.0%. Starting January 1, 2014, Phase II of the regulation required distillate fuels at or below 0.1% sulfur.

Compliance with the NA-ECA and CA-CFR are expected to come predominantly through fuel switching to lower sulfur liquid fuels. However, utilization of liquefied natural gas or SOx scrubbing may also be means by which vessel operators seek to meet the regulatory requirement. Regardless of the methods used, all are expected to result in significant reductions in $PM_{2.5}$ from marine vessels.

Previous Positive Matrix Factorization (PMF) receptor modeling studies have demonstrated the ability to quantify the contribution of marine vessel RFO combustion to $PM_{2.5}$ (Kotchenruther, 2013, 2015; and references therein) and quantified $PM_{2.5}$ reductions that occurred along the U.S. West Coast as a result of implementing the initial phases of the NA-ECA and CA-CFR (Kotchenruther, 2015). In this work, $PM_{2.5}$ from U.S. monitoring sites along the East, West, and Gulf coasts of the U.S. are analyzed spanning a period from 2010 through 2015, which includes a year or more of data through each phase of the NA-ECA regulation (unregulated, 1.0% sulfur, and 0.1% sulfur limit). PMF receptor modeling is used to quantify the $PM_{2.5}$ contribution from marine vessel RFO combustion, and statistical analysis is used to determine if changes in the contribution of RFO combustion to $PM_{2.5}$, as a result of NA-ECA implementation, are statistically significant.

2. Methods

2.1. Chemically speciated $PM_{2.5}$ data

Chemically speciated $PM_{2.5}$ data were obtained from the Interagency Monitoring of Protected Visual Environments (IMPROVE) Network. IMPROVE samplers collect 24-h integrated $PM_{2.5}$ mass and are operated on a once every third day schedule. Information about the IMPROVE network can be found on the IMPROVE web site (http://vista.cira.colostate.edu/improve/).

Data were analyzed from January 1, 2010 through December 31, 2015. This data record includes three distinct periods with respect to marine vessel fuel sulfur regulations from the NA-ECA; a 31 month period (1/2010 to 7/2012) prior to implementation of the NA-ECA (2.7% world-wide sulfur average), a 29 month period (8/2012 to 12/2014) after implementation of the initial phase of the NA-ECA (1.0% fuel sulfur limit), and a 12 month period (1/2015 to 12/2015) after implementation of the second phase of the NA-ECA (0.1% sulfur limit). These three time periods will be subsequently referred to as the pre-NA-ECA, NA-ECA 1.0% S, and NA-ECA 0.1% S, respectively.

2.2. Monitoring site selection

All IMPROVE sites in U.S. States along the West, East, and Gulf coasts as well as Hawaii were considered for PMF analysis as long as sites had a monitoring record spanning the full study period. The geographic distribution of sites considered within the continental U.S. is shown in Fig. 1, and information about the resulting 65 IMPROVE sites is listed in a table in the Supplemental materials. Of the 65 sites initially considered, site selection for PMF modeling was further narrowed based on vanadium (V) and nickel (Ni) correlation coefficients (r^2). V and Ni are well known trace metals associated with RFO combustion emissions, with V:Ni emission ratios in marine vessel RFO combustion tests typically ranging between 2 and 4.5 (Popovicheva et al., 2012; Agrawal et al., 2008). V and Ni linear r^2 and best fit slopes were computed for the 65 sites based on data from 2010 to 2011, the two years prior to implementation of the NA-ECA. A table listing the V and Ni linear r^2 and best fit slopes for these sites is provided in the Supplemental materials. Sites were selected for PMF analysis if the V:Ni r^2 was greater than 0.65. This resulted in 22 IMPROVE sites, which are listed in Table 1 and identified in Fig. 1. The V:Ni linear best fit slopes for these 22 sites ranged between 2.2 and 4.1, which is consistent with reported V:Ni emissions ratios for marine vessel RFO combustion. For each of the sites listed in Table 1, 48 h back-trajectories were computed for the ten days with highest V + Ni concentrations in 2010 and 2011 using the HYSPLIT model (Stein et al., 2015). These trajectories are provided in the Supplemental materials and demonstrate that air with high V + Ni impacting the sites on these days was overwhelmingly of marine origin, further suggesting a marine vessel origin for the V and Ni.
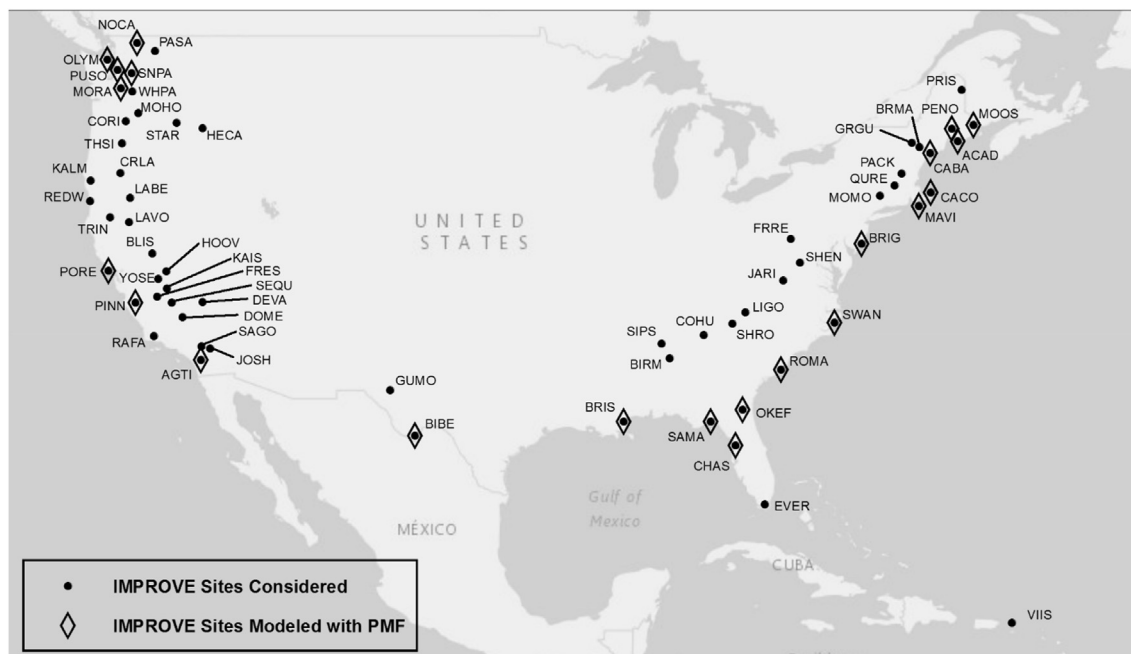
Fig. 1. IMPROVE sites used in this analysis.

2.3. Data preparation and treatment

IMPROVE datasets were processed to correct for missing or negative values, data completeness issues, and species double counting. A detailed discussion of these data preparations is provided in a previous publication by Kotchenruther (2015) and briefly summarized here. Chemical species were omitted in PMF modeling if more than 40% of samples had missing data. For remaining chemical species, missing values were replaced with median concentrations and the uncertainty set to a very high value compared to measured data, typically four times the species median concentration, to minimize the influence of the replaced data on the model solution. Any negative concentrations were reset to zero.

The uncertainty of each measurement was estimated based on the measured analytical uncertainty plus 1/3 of the method detection limit. The signal-to-noise (S/N) ratio was also used to evaluate whether chemical species should be included in the PMF modeling, and was used to adjust the data uncertainty. Chemical species were omitted in PMF modeling if the S/N ratio was less than 0.5. For chemical species with S/N between 0.5 and 1.0, data uncertainties were multiplied by a factor of 3 to down-weight the influence of these species in the model solution (Norris et al., 2014). For chlorine, measured in the IMPROVE network by both elemental (Cl) and ion analyses (Cl-), Cl-data was used because of better S/N ratios and Cl not used to avoid double counting. Also, the reported lowest temperature fraction of EC, EC1, is actually the sum of pyrolyzed

Table 1
IMPROVE monitoring sites modeled with PMF in this study.

IMPROVE site name	Abbreviation	State	Latitude	Longitude	Elevation (m)
U.S. West Coast Sites					
North Cascades	NOCA	WA	48.7316	−121.0646	569
Olympic	OLYM	WA	48.0065	−122.9727	600
Puget Sound	PUSO	WA	47.5696	−122.3119	98
Snoqualmie Pass	SNPA	WA	47.4220	−121.4259	1 049
Mount Rainier NP	MORA	WA	46.7583	−122.1244	439
Point Reyes National Seashore	PORE	CA	38.1224	−122.9085	97
Pinnacles NM	PINN	CA	36.4833	−121.1568	302
Agua Tibia	AGTI	CA	33.4636	−116.9706	508
U.S. Gulf Coast Sites					
Big Bend NP	BIBE	TX	29.3027	−103.1780	1 067
Breton Island	BRIS	LA	30.1086	−89.7617	−7
St. Marks	SAMA	FL	30.0926	−84.1614	8
Chassahowitzka NWR	CHAS	FL	28.7484	−82.5549	4
U.S. East Coast Sites					
Moosehorn NWR	MOOS	ME	45.1259	−67.2661	78
Penobscot	PENO	ME	44.9480	−68.6479	45
Acadia NP	ACAD	ME	44.3771	−68.2610	157
Casco Bay	CABA	ME	43.8325	−70.0644	27
Cape Cod	CACO	MA	41.9758	−70.0242	49
Martha's Vineyard	MAVI	MA	41.3309	−70.7846	3
Brigantine NWR	BRIG	NJ	39.4650	−74.4492	5
Swanquarter	SWAN	NC	35.4510	−76.2075	−4
Cape Romain NWR	ROMA	SC	32.9410	−79.6572	5
Okefenokee NWR	OKEF	GA	30.7405	−82.1283	48

organic carbon (OP) and low temperature combusting EC. Hence, EC1 was recalculated as EC1-OP and the measured OP value was used, so as not to double count measured OP.

2.4. Source apportionment

Source apportionment modeling was performed using EPA PMF 5.0 (Norris et al., 2014). A discussion of the mathematical equations underlying EPA PMF can be found in Paatero and Hopke (2003) and Norris et al. (2014). Data from each monitoring site was modeled independently. In each case, the model was run in the robust mode with 20 repeat runs to insure the model least-squares solution represented a global rather than local minimum and the rotational F_{PEAK} variable was held at the default value of 0.0. The model solution with the optimum number of factors was determined somewhat subjectively and was based on inspection of the factors in each solution, the quality of the least-squares fit (analysis of Q_{Robust} and Q_{True} values), and the results from three error estimation methods available in PMF 5.0; bootstrapping (BS), displacement (DISP), and bootstrapping with displacement (BS-DISP) (Norris et al., 2014; Paatero et al., 2014). The scaled residuals for final model solutions were generally normally distributed, falling into the recommended range of +3 to −3.

PMF factors can represent a single source or source category (e.g., RFO combustion, wood burning), a chemical composition (e.g., ammonium nitrate, sea salt), or mixtures of sources and compositions. During PMF modeling of each of the 22 sites in this work, it was sometimes the case that the solution that appeared to present the best delineation of sources and compositions, was in fact shown to have too much solution instability after analysis with DISP, BS, and BS-DISP (e.g., factor swaps; Brown et al., 2015). In cases like this, reducing the number of factors often led to improved solution stability, but also caused some factors to combine and become mixtures of sources, or sources and compositions. Preference in PMF solutions was given to the number of factors with improved solution stability, even if that lead to reduced source delineation. Further information on how the model solution with the optimal number of factors was selected is provided in the Supplemental materials.

3. Results and discussion

3.1. Identified PM$_{2.5}$ sources and compositions

PMF modeling for each of the 22 sites resulted in solutions with from 5 to 9 factors, depending on the site. Table 2 lists the 12 different sources and compositions that were identified at the 22 sites, at how many sites each source or composition was identified,

and how often they were identified in a factor by themselves versus in a factor mixed with other sources or compositions. A table in the Supplemental materials lists each site, the number of factors found, and the factor attributions using the source or composition identifiers listed in Table 2. PMF factor mass time series and factor chemical profiles for each site are also provided in the Supplemental materials. The chemical profiles presented in the Supplemental materials are those after the factor chemical composition from each site was normalized. A factor chemical composition was normalized by first assuming an organic mass (OMC) to OC ratio of 1.8 (i.e., multiplying all OC fraction by 1.8). An OMC to OC ratio of 1.8 is a common ratio used for rural and remote monitoring sites and is used to account for the full mass of organic material, not just the carbon portion. Second, in order to fully account for all sulfate and nitrate mass, sulfate and nitrate were assumed to be fully neutralized and present as ammonium sulfate and ammonium nitrate. Ammonium ion is not measured in the IMPROVE network, but given the rural and remote locations of most monitors, full neutralization is a reasonable assumption. Third, to fully account for the mass of fugitive dust, for factors associated with fugitive dust a metal oxide to metal ratio was assumed for aluminum (Al, ratio of 2.2), calcium (Ca, 1.63), iron (Fe, 2.42), titanium (Ti, 1.94), and silicon (Si, 2.49) based on the ratios used in the IMPROVE network (Solomon et al., 2014). Lastly, all of these components and the remaining measured species were summed and each chemical component was divided by the sum to normalize the chemical profile. Presenting the normalized chemical profiles gives a better representation of the importance of each chemical species to the overall profile, and is needed for profile comparisons across multiple sites.

The sources and compositions listed in Table 2 were identified by comparing the chemical composition of PMF factors with chemical profiles in EPA's SPECIATE database of source emissions test data (https://www3.epa.gov/ttnchie1/software/speciate/), comparison with similar PMF factor chemical compositions identified in existing published studies, knowledge of the seasonal emissions patterns of aerosol sources, and composition of aerosols found in the natural environment (e.g., fugitive dust, sea salt). The sections below describe how each source or composition was identified, and for the 7 most commonly found, Fig. 2 depicts the average PMF factor chemical profile from multiple sites. Average profiles were calculated only from those factors that were determined not to be a mixture. The number of individual profiles making up the average profiles in Fig. 2 ranged from 6 to 21, and depended on how well resolved the source or composition was in the modeling results across all sites. Data tables for the average profiles are provided in the Supplemental materials. The average factor profiles were taken after the PMF factor chemical profile

Table 2
Sources and chemical compositions identified by PMF, and the number of sites where appearing as a single PMF factor, or in a factor mixed with other listed sources or chemical compositions.

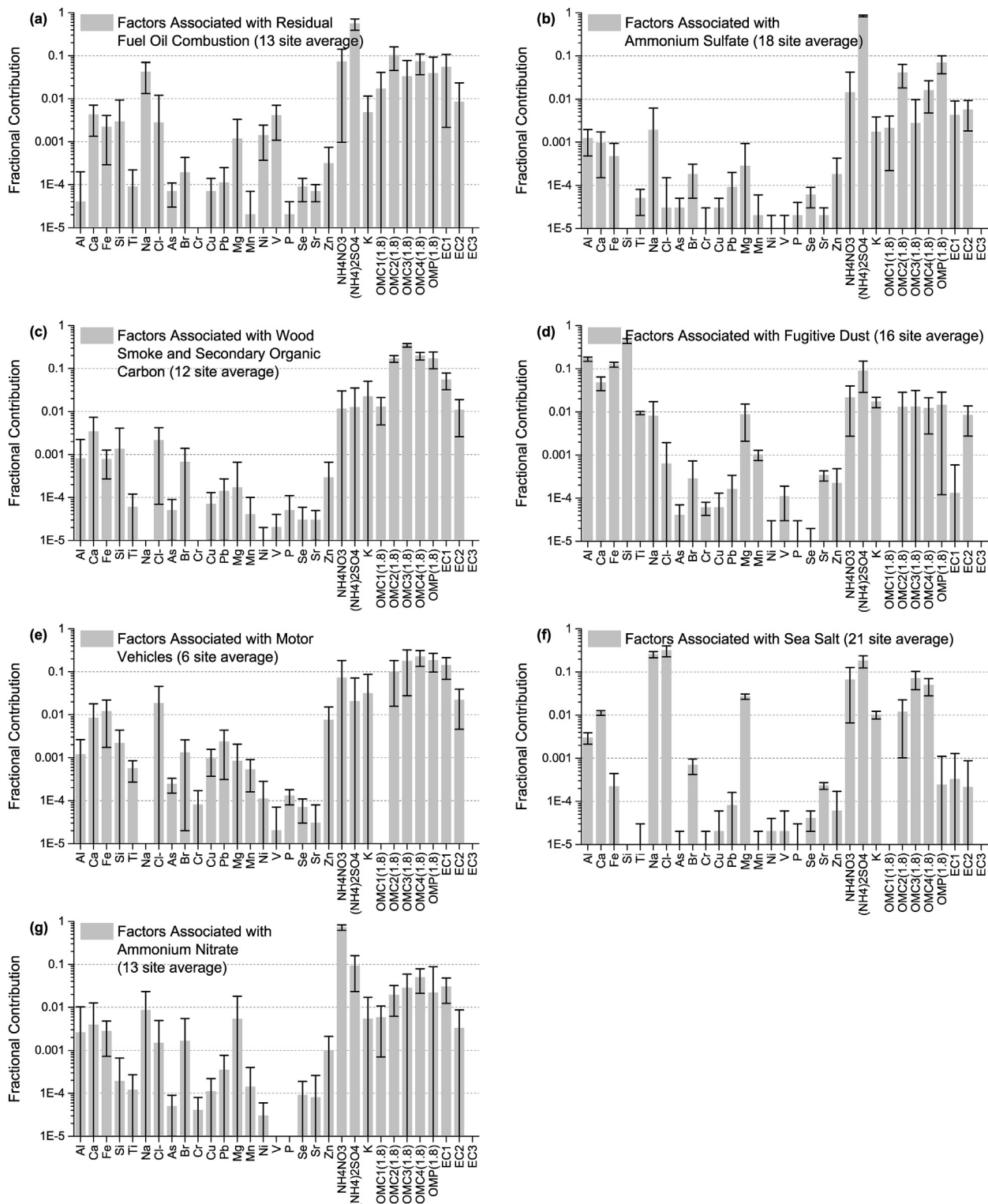| Source or composition identifier	Identified source or composition	Number of sites where appears	Number of sites where a single factor	Number of sites where in a mixed factor
1	Residual Fuel Oil Combustion	22	13	9
2	Ammonium Sulfate	22	18	4
3	Wood Smoke and Secondary Organic Carbon	22	12	10
4	Fugitive Dust	22	16	6
5	Motor Vehicles	21	6	15
6	Sea Salt	21	21	0
7	Ammonium Nitrate	19	13	6
8	Aged Sea Salt	5	1	4
9	Potassium Rich Ammonium Sulfate	5	2	3
10	Unidentified Organic Aerosol	4	1	3
11	Calcium Rich Fugitive Dust	1	1	0
12	Iron Rich	1	1	0

Fig. 2. Average and standard deviation of chemical profiles from PMF factors from multiple sites associated with (a) residual fuel oil combustion, (b) ammonium sulfate, (c) wood smoke and secondary OC, (d) fugitive dust, (e) motor vehicles, (f) sea salt, and (g) ammonium nitrate.

from each site was normalized as described above. Average profiles offer a more robust representation of the chemical composition of an aerosol source than do results from a single PMF solution, and could be useful for comparison to other source apportionment analyses, or even used as source profile inputs in Chemical Mass Balance receptor modeling.

3.1.1. PMF factors associated with residual fuel oil combustion

A PMF factor containing RFO combustion was identified at all 22 sites modeled. This was expected because these sites were chosen based on strong V:Ni correlations and had correlation slopes in the ambient data similar to marine vessel RFO emissions ratios. At 9 sites, inspection of the chemical composition of the factor

associated with RFO combustion resulted in the determination that the factor represented a mixture of other sources in addition to RFO combustion. At the 13 remaining sites, the factor associated with RFO combustion was judged not to be mixed with other sources. At these 13 sites, the V:Ni ratio in the PMF chemical profiles ranged from 2.4 to 3.9 with an average value of 2.9. These V:Ni ratios were similar that from the ambient measurements, which ranged from 2.2 to 3.7 with an average of 3.0 (see Supplemental materials) and are similar to ratios found in Kotchenruther (2015). The average chemical profile from PMF factors at these 13 sites is shown in Fig. 2a.

Other than several categories of stationary sources, no other significant sources of V and Ni have V:Ni emissions ratios above 1.0 in the EPA SPECIATE database. While contributions from stationary sources cannot be completely ruled out, the coastal and remote locations of most sites considered here, along with the marine origin of back-trajectories on high V + Ni monitored days in 2010−2011, suggests RFO combustion from marine vessels is the likely dominant source of V and Ni.

Sulfate is an important component of all PMF factors that were associated with RFO combustion. However, sulfate is a ubiquitous component of ambient $PM_{2.5}$ whenever chemical speciation of $PM_{2.5}$ is performed, and there are often many sources of environmental sulfate. In order to ensure that changes in RFO combustion factor concentrations were not associated with changes in emissions from other sources of environmental sulfate, model results for marine vessel RFO combustion are only used to analyze the effect of the NA-ECA if PMF modeling passed acceptable performance criteria from all three uncertainty estimation methods (BS, DISP, and BS-DISP) recommended in the PMF 5.0 user's guide (Norris et al., 2014) and a separate ammonium sulfate factor was found at that site. A previous publication (Kotchenruther, 2015) demonstrated that when these criteria were met, statistically significant changes in the contribution of RFO combustion to $PM_{2.5}$ only occurred in areas where fuel sulfur was being regulated, even though all sites had shown a statistically significant reduction in ambient sulfate. This gave confidence in the previous published results that changes in the contribution of RFO combustion to $PM_{2.5}$ identified by PMF were not associated with sulfur reduction measures implemented in other source sectors. Adhering to the same performance criteria in this work bolsters a similar confidence.

For 4 of the 9 sites mentioned above where RFO combustion was found to be part of a factor mixed with other sources, this determination was made because no separate factors were identified containing secondary sulfate. In these cases, it was assumed that the sulfate component of the factor associated with RFO combustion represented multiple sources of environmental sulfate, not just from RFO combustion. Hence, these factors were deemed to be from a mixture of sources. At 3 of the 9 sites, RFO combustion was determined to be mixed with other sources of organic aerosol, and at 2 of the 9 sites RFO combustion was determined to be mixed with aged sea salt.

3.1.2. PMF factors associated with ammonium sulfate

The main chemical constituent in this factor was sulfate and was assumed to be fully neutralized by ammonium. This factor typically had a seasonal pattern of higher mass attributions in summer months. The average chemical profile from PMF factors at 18 sites where this source was not mixed with other sources is shown in Fig. 2b.

3.1.3. PMF factors associated with wood smoke and secondary organic carbon

A factor mixing secondary organic aerosol with wood smoke emissions. This factor occurred, unmixed with other sources, at 12 sites and was characterized by a chemical profile dominated by organic carbon (OC), elemental carbon (EC), and potassium and a $PM_{2.5}$ mass time series at most sites having occasional spikes above 5 μg/m3 on top of continuous contributions between 0.5 and 1 μg/m3. The average chemical profile from PMF factors at 12 sites where this source was not mixed with other sources is shown in Fig. 2c.

3.1.4. PMF factors associated with fugitive dust

The principal chemical constituents in this factor were Al, Ca, Fe, and Si. Significant trace constituents were Ti and K. The typical seasonal pattern of mass is higher in late summer and lower in winter and spring and corresponds to the typical seasons with less and more precipitation, respectively. The average chemical profile from PMF factors at 16 sites where this source was not mixed with other sources is shown in Fig. 2d. The fractional contributions of the principal and trace chemical constituents in the average profile are similar to that of numerous soil dust profiles in EPA's SPECIATE database.

3.1.5. PMF factors associated with motor vehicles

The principal chemical constituents in this factor were EC1, OC2, OC3, OC4, and OP. Significant trace constituents were zinc (Zn), lead (Pb), copper (Cu), and Fe. The average chemical profile from PMF factors at 6 sites where this source was not mixed with other sources is shown in Fig. 2e. The dominant chemical constituents are similar to those found for motor vehicles in previous publications (Zhao and Hopke, 2004; Kim and Hopke, 2006; Hwang and Hopke, 2007). The significant trace metal constituents match those commonly found in $PM_{2.5}$ associated with motor vehicles (Song and Gao, 2011; Pant and Harrison, 2013). These factors represent a mixture of vehicle exhaust and non-exhaust (e.g., tire wear) emissions. The near ubiquity of this source at the sites in this study matches the conceptual understanding of motor vehicles as a common source of particulate pollution. Separate factors for gasoline and diesel vehicles were not found in this study, and this factor likely represents a combination of these sources.

3.1.6. PMF factors associated with sea salt

This factor was dominated by Na and Cl. Significant trace constituents were magnesium (Mg) and Ca. Mass impacts for this factor had no discernable seasonal pattern, suggesting these factors are from natural sources rather than winter road salting. The average chemical profile from PMF factors at 21 sites where this source was not mixed with other sources is shown in Fig. 2f.

3.1.7. PMF factors associated with ammonium nitrate

The main chemical constituent in this factor was nitrate and was assumed to be fully neutralized by ammonium. The typical seasonal pattern of mass impacts showed high winter and low summer impacts, which is indicative of secondary formation, and likely from multiple sources of NO_x. The average chemical profile from PMF factors at 13 sites where this source was not mixed with other sources is shown in Fig. 2g.

3.1.8. PMF factors associated with aged sea salt

This factor had the same identifying features as Sea Salt, but with little or no Cl and the addition of a significant contribution from nitrate. The replacement of Cl with nitrate is typical of sea salt after aging (Adachi and Buseck, 2015).

3.1.9. PMF factors associated with potassium rich ammonium sulfate

The main chemical constituent in this factor was sulfate with a significant contribution from potassium. Sulfate was assumed to be fully neutralized by ammonium.

3.1.10. PMF factors associated with unidentified organic aerosol

This classification was given to factors that contained a significant amount of organic mass that could not otherwise be identified. Most factors showed higher concentrations in summer, which could indicate an association with secondary organic aerosol. 4 of the 22 sites had factors like this.

3.1.11. PMF factors associated with calcium rich fugitive dust

This factor was similar to fugitive dust, but with a significantly higher calcium concentration than the typical fugitive dust chemical profile.

3.1.12. PMF factors associated with iron rich

This factor was dominated by Fe, OC2, OC3, OC4, and EC1. Significant trace constituents were chromium, Cu, Zn, and manganese. This factor was only found in Seattle. It is likely this factor is related to metal fabrication or other industrial activity.

3.2. PMF results and NA-ECA effectiveness at reducing RFO combustion from marine vessels

The effectiveness of the NA-ECA at reducing contributions from marine vessel RFO combustion to PM$_{2.5}$ was assessed at the 13 sites where PMF results indicated a well delineated factor associated with RFO combustion (see Section 2.4 above). NA-ECA effectiveness could not be easily assessed at those 9 sites where mixed factors containing RFO combustion were identified. NA-ECA effectiveness was assessed by determining if statistically significant reductions in PM$_{2.5}$ from RFO combustion had occurred. Significance testing was performed using the nonparametric Wilcoxon-Mann-Whitney (WMW) test (ProUCL version 5.0; https://www.epa.gov/land-research/proucl-software).

The distribution of mass impacts for PMF factors associated with RFO combustion was compared between three time periods associated with differing NA-ECA fuel sulfur regulation; 24 months (1/2010 to 12/2011) in the pre-NA-ECA period, 24 months (1/2013 to 12/2014) in the NA-ECA 1.0% S period, and 12 months (1/2015 to 12/2015) in the NA-ECA 0.1% S period. Full annual time periods were compared in the statistical analyses, either 12 or 24 months, because PMF factors associated with RFO combustion at many sites had a pronounced seasonal cycle with higher summer values and lower winter values. This seasonal cycle can be explained by increased stability in the summertime marine boundary layer compared to winter. The heightened stability in the summer marine boundary layer more efficiently traps marine vessel exhaust plumes, and as these plumes transition from over water to over land they undergo coastal fumigation. Because a similar seasonal cycle is observed in the ambient V and Ni measurements, the seasonal cycle is not thought to be significantly related to elevated secondary production of sulfate in summer. However, increased summertime marine vessel activity may contribute to the observed season cycle in some locations, such as locations impacted by seasonal cruise ship activity.

Fig. 3 shows three examples of time series of PMF factors associated with RFO combustion, the PM$_{2.5}$ from RFO combustion at OLYM, BRIS, and CACO IMPROVE monitoring sites. Decreases in PM$_{2.5}$ mass from RFO combustion are apparent in each period of the NA-ECA regulation. Time series of mass impacts for all factors can be found in the Supplemental materials.

Table 3 shows the annualized (the average of 24 or 12 monthly averages) average RFO mass contribution to PM$_{2.5}$ at the 13 IMPROVE sites for the pre-NA-ECA, NA-ECA 1.0% S, and NA-ECA 0.1% S periods. Table 3, Fig. 4, and Fig. 5 show the percent change in annualized average RFO mass from the pre-NA-ECA to NA-ECA 1% S periods and from the pre-NA-ECA to NA-ECA 0.1% S periods.

Changes in RFO mass between these periods were all found to be statistically significant at the 99% confidence interval using the WMW test.

To isolate the effect of the NA-ECA regulation from the CA-CFR regulation, results for the 2 sites in CA were excluded. For the remaining 11 sites, the average decrease in PM$_{2.5}$ from RFO combustion was 50.2% from the pre-NA-ECA to NA-ECA 1% S period and 74.1% from the pre-NA-ECA to NA-ECA 0.1% S period.

Decreases in PM$_{2.5}$, from the pre-NA-ECA baseline period of 2010–2011 to the NA-ECA 0.1% S period in 2015, were greater than 77.2% at every site except for the two U.S. Gulf Coast IMPROVE sites of SAMA and CHAS, which only showed reductions of 33.0% and 35.4%, respectively. It is unclear why these two sites did not see similar reductions as the other sites. Potential explanations include that there may be other sources of RFO combustion besides marine vessels that are impacting these sites, that there may be lax compliance with the NA-ECA in this region, or that the ECA zone near the southeastern Florida coast narrows to much less than 200 nm because the ECA cannot be enforced in the territorial waters of other counties. Hence, unregulated emissions outside of that narrowed ECA zone may be impacting these sites. Further study and tracking is recommended.

3.3. Other possible factors influencing the PMF results for changes in annual PM$_{2.5}$ from RFO combustion

In addition to the implementation of marine vessel fuel sulfur regulations, annual changes in marine vessel traffic could affect the amount of marine vessel PM$_{2.5}$ contributing to ambient monitors. To address this concern, data for annual waterborne shipping tonnage in U.S. costal states and annual shipping container traffic volume at major ports were analyzed from 2010 to the latest year of available data, 2014 (US Army Corps of Engineers, 2016). Both data sets showed that annual ship traffic was relatively steady over the 5-year period. Data tables for shipping tonnage and shipping container traffic are provided in the Supplemental data. In regards to passenger vessel traffic such as from cruise ships, annual cruise ship port calls in many ports have also remained relatively constant in the 2010–2015 period covered in this study (e.g., Port of Seattle, 2016; Port Tampa Bay, 2016).

The chemical composition of fuels used by ocean-going vessels can also vary. This study assumes that, in the absence of fuel sulfur regulations, most marine vessels capable of using RFO fuels will do so because of the low cost. However, RFO is a general term for residual fuels that can have varying chemical compositions. While the global average sulfur content of RFO used by marine vessels has been relatively stable between 2.6 and 2.7% in recent years, the sulfur content of RFO on individual ships can vary depending on the fuels' source region (IMO, 2011). The V and Ni concentrations in RFO can span a wide range (Kasper et al., 2007; Khan et al., 2012), however, as noted above the V to Ni ratio in RFO combustion tests typically ranges between 2 and 4.5. While temporal changes in the chemical composition of RFO used along the U.S. coasts could not be determined with available data sources, given that the global average sulfur content has been relatively stable during the time period of this study, it is likely that chemical composition changes implemented to meet the fuel sulfur regulations are significantly larger than the temporal fluctuations in average RFO chemical composition used in the U.S. coastal regions.

Change in meteorology between the years analyzed in this study is also a source of potential variability effecting these results. The most influential meteorological variables are likely precipitation, wind speed, wind direction, and factors effecting coastal fumigation dynamics. However, given the temporal and geographic scope
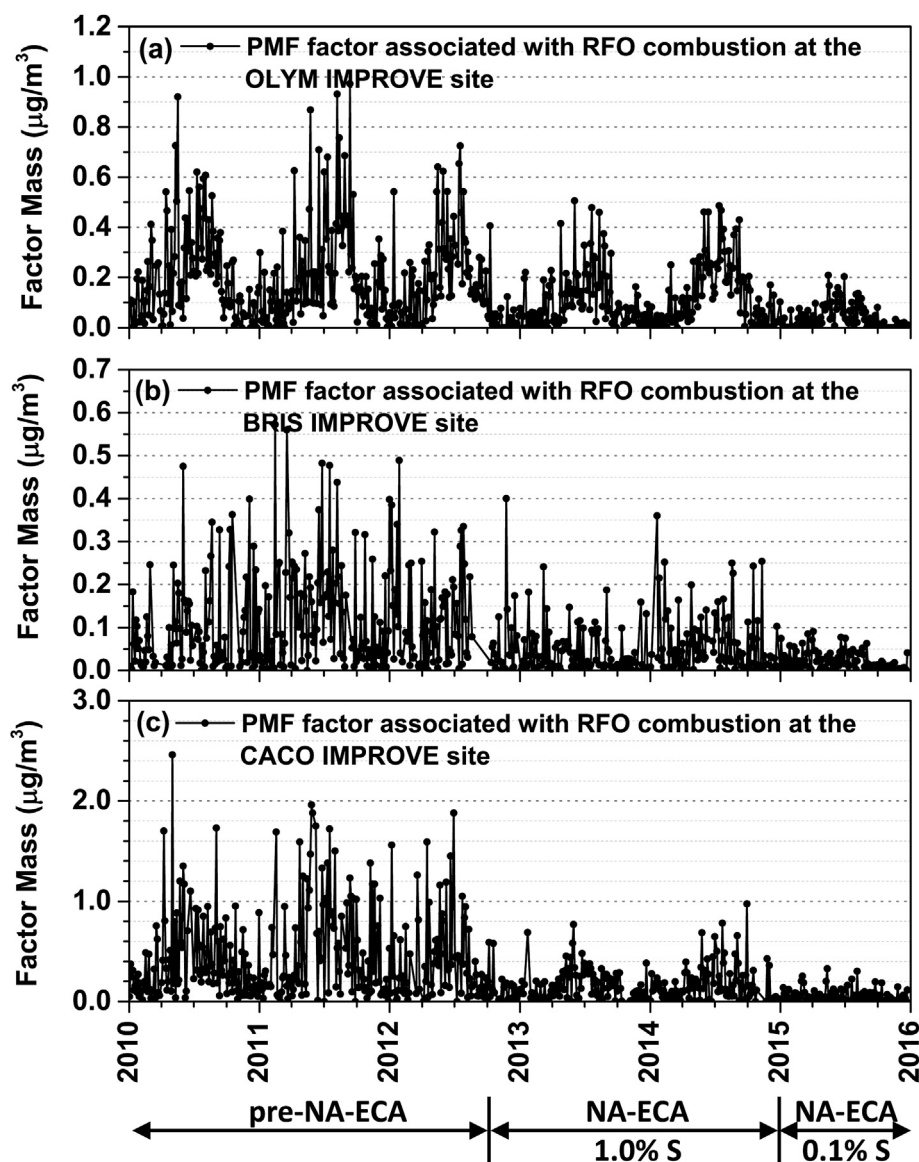
Fig. 3. Time series of PMF factors associated with RFO combustion at the OLYM, BRIS, and CACO IMPROVE monitoring sites.

Table 3
Annualized average RFO combustion emissions contribution to $PM_{2.5}$ for the pre-NA-ECA, NA-ECA 1% S, and NA-ECA 0.1% S periods and percent change in RFO combustion emissions contribution between the annualized average periods.

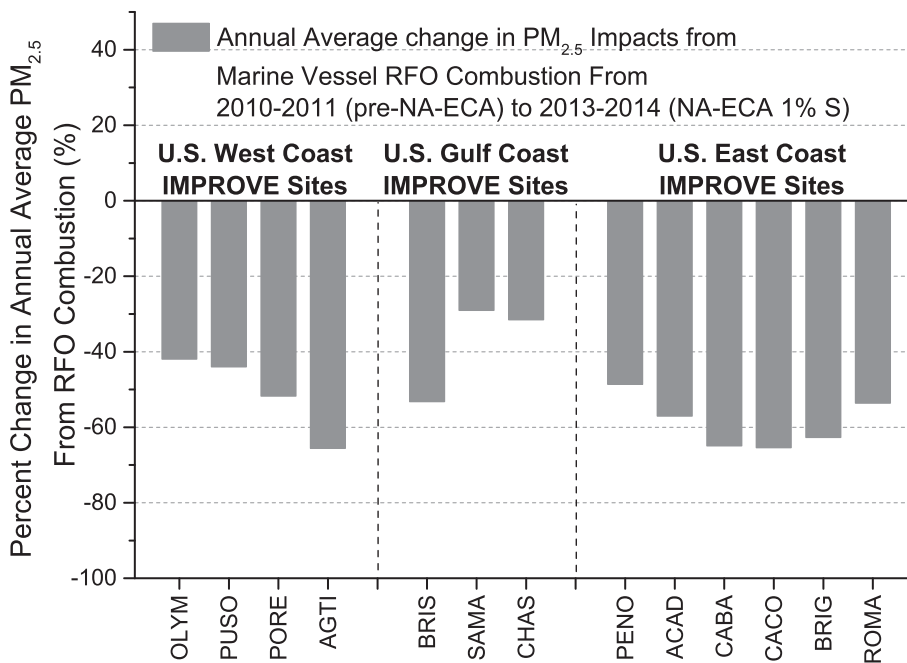| IMPROVE monitor abbreviation	pre-NA-ECA (2010—2011) RFO mass (µg/m3)	NA-ECA 1% S (2013—2014) RFO mass (µg/m3)	NA-ECA 0.1% S (2015) RFO mass (µg/m3)	pre-NA-ECA to NA-ECA 1% S RFO mass change (%)	pre-NA-ECA to NA-ECA 0.1% S RFO mass change (%)
U.S. West Coast Sites					
OLYM	0.205	0.119	0.039	−41.9	−81.0
PUSO	0.511	0.286	0.104	−44.0	−79.7
PORE	0.005	0.003	0.001	−51.7	−81.6
AGTI	0.235	0.081	0.040	−65.6	−83.0
U.S. Gulf Coast Sites					
BRIS	0.108	0.051	0.021	−53.2	−80.9
SAMA	1.124	0.797	0.753	−29.0	−33.0
CHAS	0.806	0.552	0.521	−31.5	−35.4
U.S. East Coast Sites					
PENO	0.060	0.031	0.009	−48.6	−84.4
ACAD	0.019	0.008	0.002	−57.0	−87.4
CABA	0.735	0.258	0.167	−64.9	−77.3
CACO	0.459	0.159	0.053	−65.4	−88.6
BRIG	0.454	0.169	0.044	−62.7	−90.4
ROMA	0.916	0.425	0.209	−53.6	−77.2

Fig. 4. Percent change in annual average PM$_{2.5}$ from marine vessel RFO combustion from the pre-NA-ECA (2010–2011) to NA-ECA 1% S (2013–2014) periods.
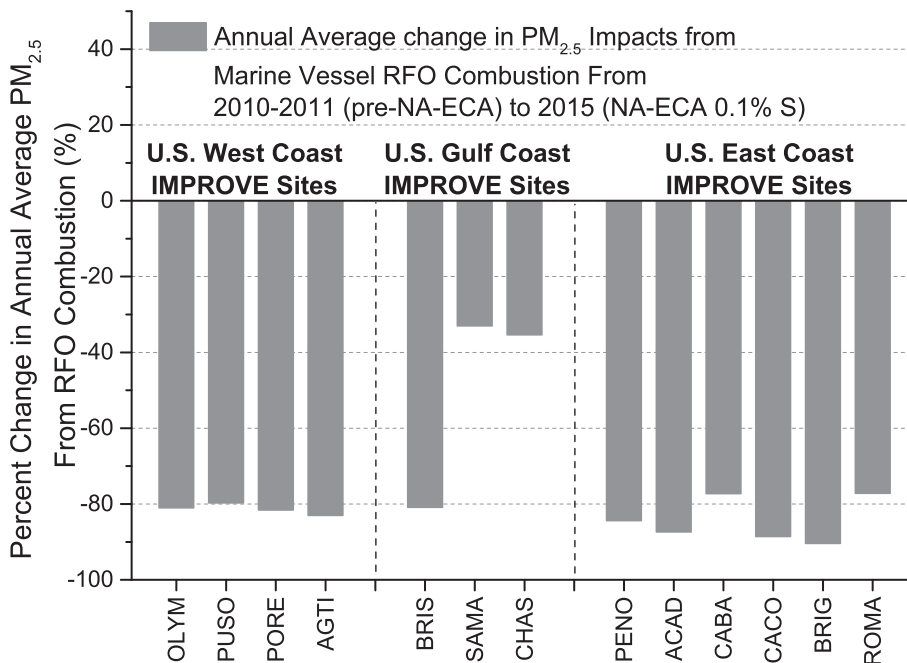

Fig. 5. Percent change in annual average PM$_{2.5}$ from marine vessel RFO combustion from the pre-NA-ECA (2010–2011) to NA-ECA 0.1% S (2015) periods.

of this work, a detailed meteorological analysis for each site is beyond the scope of this study.

4. Conclusions

This work uses ambient PM$_{2.5}$ monitoring data from the U.S. IMPROVE network and PMF receptor modeling to assess the effectiveness of the NA-ECA at reducing ambient PM$_{2.5}$ from marine vessel RFO combustion. V and Ni data from 65 IMPROVE sites in coastal States of the U.S. were analyzed to identify sites with PM$_{2.5}$ contributions from RFO combustion, and 22 of these sites were selected for PMF receptor modeling. Each site was modeled independently with PMF, obtaining from 5 to 9 factors depending on the site. Every site resolved a PMF factor associated with RFO combustion, but these factors at some sites contained RFO combustion mixed with other aerosol sources. 13 sites were deemed to have PMF factors associated with RFO combustion that were not mixed with other sources. For these 13 sites, PM$_{2.5}$ from RFO combustion

was analyzed for three time periods related to various levels of fuel sulfur control under the NA-ECA; pre-NA-ECA, NA-ECA 1.0% S, and NA-ECA 0.1% S. Implementation of the NA-ECA was found to be effective at reducing $PM_{2.5}$ from RFO combustion, with all 13 sites indicating statistically significant reductions in $PM_{2.5}$ from RFO combustion between the pre-NA-ECA period and the two periods of fuel sulfur control. The average decrease in annual average $PM_{2.5}$ from RFO combustion resulting from the NA-ECA implementation was 50.2% from the pre-NA-ECA to NA-ECA 1% S period and 74.1% from the pre-NA-ECA to NA-ECA 0.1% S period.

Appendix A. Supplementary data

Supplementary data related to this article can be found at http://dx.doi.org/10.1016/j.atmosenv.2016.12.012.

References

Adachi, K., Buseck, P.R., 2015. Changes in shape and composition of sea-salt particles upon aging in an urban atmosphere. Atmos. Environ. 100, 1—9.

Agrawal, H., Malloy, Q.G.J., Welch, W.A., Miller, J.W., Cocker III, D.R., 2008. In-use gaseous and particulate matter emissions from a modern ocean going container vessel. Atmos. Environ. 42, 5504—5510.

Brown, S.G., Eberly, S., Paatero, P., Norris, G.A., 2015. Methods for estimating uncertainty in PMF solutions: examples with ambient air and water quality data and guidance on reporting PMF results. Sci. Total Environ. 518—519, 626—635.

Corbett, J.J., Winebrake, J.J., Green, E.H., Kasibhatla, P., Eyring, V., Lauer, A., 2007. Mortality from ship emissions: a global assessment. Environ. Sci. Technol. 41, 8512—8518.

Geiser, L.H., Jovan, S.E., Glavich, D.A., Porter, M.K., 2010. Lichen based critical loads for atmospheric nitrogen deposition in Western Oregon and Washington Forests, USA. Environ. Pollut. 158, 2412—2421.

Hwang, I., Hopke, P.K., 2007. Estimation of source apportionment and potential source locations of $PM_{2.5}$ at a west coastal IMPROVE site. Atmos. Environ. 41, 506—518.

IMO, 2011. Prevention of Air Pollution from Ships: Sulphur Monitoring for 2010. International Maritime Organization Marine Environment Protection Committee. MEPC 62/4.

IPCC, 2014. Climate change 2014: synthesis report. Core Writing Team. In: Pachauri, R.K., Meyer, L.A. (Eds.), Contribution of Working Groups I, II and III to the Fifth Assessment Report of the Intergovernmental Panel on Climate Change. IPCC, Geneva, Switzerland, 151 pp.

Kasper, A., Aufdenblatten, S., Forss, A., Mohr, M., Burtscher, H., 2007. Particulate emissions from a low-speed marine diesel engine. Aerosol Sci. Technol. 41, 24—32.

Khan, M.Y., Giordano, M., Gutierrez, J., Welch, W.A., Asa-Awuku, A., Miller, J.W., Cocker III, D.R., 2012. Benefits of two mitigation strategies for container vessels: cleaner engines and cleaner fuels. Environ. Sci. Technol. 46, 5049—5056.

Kim, E., Hopke, P.K., 2006. Characterization of fine particle sources in the Great Smoky Mountains area. Sci. Total Environ. 368, 781—794.

Kotchenruther, R.A., 2013. A regional assessment of marine vessel $PM_{2.5}$ impacts in the U.S. Pacific Northwest using a receptor-based source apportionment method. Atmos. Environ. 68, 103—111.

Kotchenruther, R.A., 2015. The effects of marine vessel fuel sulfur regulations on ambient $PM_{2.5}$ along the west coast of the U.S. Atmos. Environ. 103, 121—128.

Künzli, N., Jerrett, M., Mack, W.J., Beckerman, B., LaBree, L., Gilliland, F., Thomas, M., Peters, J., Hodis, H.N., 2005. Ambient air pollution and atherosclerosis in Los Angeles. Environ. Health Perspect. 113, 201—206.

Moldanova, J., Fridell, E., Popovicheva, O., Demirdjian, B., Tishkova, V., Faccinetto, A., Focsa, C., 2009. Characterisation of particulate matter and gaseous emissions from a large ship diesel engine. Atmos. Environ. 43, 2632—2641.

Norris, G., Duvall, R., Brown, S., Bai, S., 2014. EPA Positive Matrix Factorization (PMF) 5.0 Fundamentals and User Guide. U.S. Environmental Protection Agency. EPA/600/R-14/108.

Paatero, P., Eberly, S., Brown, S.G., Norris, G.A., 2014. Methods for estimating uncertainty in factor analytic solutions. Atmos. Meas. Tech. 7, 781—797.

Paatero, P., Hopke, P.K., 2003. Discarding or downweighting high-noise variables in factor analytic models. Anal. Chim. Acta 490, 277—289.

Pant, P., Harrison, R.M., 2013. Estimation of the contribution of road traffic emissions to particulate matter concentrations from field measurements: a review. Atmos. Environ. 77, 78—97.

Pope III, C.A., Dockery, D.W., 2006. Health effects of fine particulate air pollution: lines that connect. J. Air & Waste Manag. Assoc. 56, 709—742.

Popovicheva, O., Kireeva, E., Persiantseva, N., Timofeev, M., Bladt, H., Ivleca, N.P., Niessner, R., Moldanova, J., 2012. Microscopic characterization of individual particles from multicomponent ship exhaust. J. Environ. Monit. 14, 3101—3110.

Port of Seattle, 2016. Cruise Seattle 2016 Fact Sheet. https://www.portseattle.org/Cruise/Documents/2016_cruise_factsheet.pdf (accessed 30 November 2016).

Port Tampa Bay, 2016. Port Tampa Bay Fiscal Years 2006-2015 Cargo and Vessel Statistics. https://www.tampaport.com/About-Port-Tampa-Bay/Statistics (accessed 30 November 2016).

Ramberg, D., Van Vactor, S., 2014. Implications of Residual Fuel Oil Phase Out. 37th International Association for Energy Economics (IAEE) International Conference, New York, NY. June 15-18, 2014.

Solomon, P.A., Crumpler, D., Flanagan, J.B., Jayanty, R.K.M., Rickman, E.E., McDade, C.E., 2014. U.S. National $PM_{2.5}$ chemical speciation monitoring networks—CSN and IMPROVE: description of networks. J. Air & Waste Manag. Assoc. 64, 1410—1438.

Song, F., Gao, Y., 2011. Size distributions of trace elements associated with ambient particular matter in the affinity of a major highway in the New Jersey-New York metropolitan area. Atmos. Environ. 45, 6714—6723.

Stein, A.F., Draxler, R.R., Rolph, G.D., Stunder, B.J.B., Cohen, M.D., Ngan, F., 2015. NOAA's HYSPLIT atmospheric transport and dispersion modeling system. Bull. Amer. Meteor. Soc. 96, 2059—2077.

U.S. Environmental Protection Agency, 2010. Designation of North American Emission Control Area to Reduce Emissions from Ships: Regulatory Announcement. EPA-420-F-10—015.

US Army Corps of Engineers, 2016. Waterborne Commerce Statistics Center. http://www.navigationdatacenter.us/wcsc/wcsc.htm (accessed 24 August 2016).

Winebrake, J.J., Corbett, J.J., Green, E.H., Lauer, A., Eyring, V., 2009. Mitigating the health impacts of pollution from oceangoing shipping: an assessment of low-sulfur fuel mandates. Environ. Sci. Technol. 43, 4776—4782.

Zhao, W., Hopke, P.K., 2004. Source apportionment for ambient particles in the San Gorgonio wilderness. Atmos. Environ. 38, 5901—5910.